Anal. Chem. **2005,** *77,* 8068−8074

Direct Electrochemistry of Myoglobin in Titanate Nanotubes Film

Aihua Liu,† Mingdeng Wei,† Itaru Honma,† and Haoshen Zhou*,†,‡

Energy Technology Research Institute, National Institute of Advanced Industrial Science and Technology (AIST), Umezono 1-1-1, Tsukuba 305-8568, Japan, and PRESTO, Japan Science and Technology Agency, Kawauchi, Saitama 332-0012, Japan

Titanate nanotubes (TNT) were proven to be efficient support matrixes for the immobilization of myoglobin (Mb). A comparative study was performed using the corresponding analogue, nanocrystalline anatase TiO_2 (TNP). UV−visible absorption and FT-IR spectra show that Mb was not obviously denatured in TNT film in contrast to the significant denaturation of Mb in TNP film. Cyclic voltammetry and square wave voltammetry measurements were carried out using the Mb−TNT or Mb−TNP cast film-covered basal plane pyrolytic graphite electrode. The Mb−TNT film gave a well-defined, nearly reversible redox couple with the apparent formal peak potential (E_p) of −0.239 V (vs Ag/AgCl) in pH 5.5 buffer, whereas a relatively smaller, quais-reversible redox pair with E_p of −0.263 V was observed for the Mb−TNP film. The amounts of electroactive Mb in TNT film and TNP film were 15 and 10%, respectively. Moreover, the Mb−TNT film exerted facile direct electron transfer with the apparent heterogeneous electron-transfer rate constant (k_{ET}) of $86 \pm 7\ s^{-1}$, almost 4 times the $22 \pm 5\ s^{-1}$ value for the Mb−TNP membrane and higher than other Mb-entrapped films reported. Additionally, the Mb−TNT film demonstrates good electrocatalytic reduction of hydrogen peroxide with a detection limit of 0.6 μM, much lower than the 3.0 μM value for the Mb−TNP electrode and other Mb-related film-modified electrodes reported so far. The Mb−TNT film exhibits higher peroxidase-like activity with the apparent Michaelis-Menton constant (K_M) of 140 μM, significantly lower than the 1300 μM value for the Mb−TNP film. The functional hydroxyl group and the surface charge as well as tubular morphology of TNT are important factors to stabilize the bound protein.

There has been increasing interest in studying metalloproteins in order to achieve direct electron transfer for applications in mediator-free biosensors, bioreactors, and mimicking catalytic roles in living systems.[1] Many electron-transfer metalloproteins are membrane-associated, and efficient electron transfer for proteins can only be accomplished within the membrane environment.[2] Myoglobin (Mb) is a single-chain protein of 153 amino acids, containing a heme (iron-containing porphyrin) group in the center. Mb is found in mammalian skeleton and muscle tissues, which functions in the storage of oxygen and in the enhancement of the rate of oxygen diffusion.[3] Because the heme group in Mb is much more buried with respect to the protein surface than in cytochrome, its interaction with the electrode surface is hindered.[4] To explore methods to increase the electron transfer between Mb and the electrode, great efforts have been devoted to the characterization of the electrochemistry of Mb using electrodes modified with films such as surfactants,[5] polymers,[6] and distal histidine.[7] Recently, the adsorption of enzymes on inorganic materials has been reported.[8−11] These films provide the friendly

* Corresponding author. E-mail: hs.zhou@aist.go.jp.
† National Institute of Advanced Industrial Science and Technology.
‡ Japan Science and Technology Agency.

(1) (a) Armstrong, F. A.; Hill, H. A. O.; Walton, N. J. *Acc. Chem. Res.* **1988**, *21*, 407−413. (b) Beissenhirtz, M. K. Scheller, F. W.; Lisdat, F. *Anal. Chem.* **2004**, *76*, 4665−4671.
(2) Hamachi, I.; Fujita, A.; Kunitake, T. *J. Am. Chem. Soc.* **1997**, *119*, 9096−9102.
(3) (a) Stargardt, J. F.; Hawkridge, F. M.; Landrum, H. L. *Anal. Chem.* **1978**, *50*, 930−932. (b) Hildebrand, D. P.; Tang, H.-l.; Luo, Y.; Hunter, C. L.; Smith, M.; Brayer, G. D.; Mauk, A. G. *J. Am. Chem. Soc.* **1996**, *118*, 12909−12915.
(4) Stellwagen, E. *Nature* **1978**, *275*, 73−74.
(5) (a) Rusling, J. F.; Nassar, A.-E. F. *J. Am. Chem. Soc.* **1993**, *115*, 11891−11897. (b) Nassar, A.-E. F.; Bobbitt, J. M.; Struart, J. D.; Rusling, J. F. *J. Am. Chem. Soc.* **1995**, *117*, 10986−10993. (c) Lin, R.; Bayachou, M.; Greaves, J.; Farmer, P. J. *J. Am. Chem. Soc.* **1997**, *119*, 12689−12690. (d) Hu, N., Rusling, J. F. *Langmuir* **1997**, *13*, 4119−4125. (e) Bayachou, M.; Lin, R.; Cho, W.; Farmer, P. J. *J. Am. Chem. Soc.* **1998**, *120*, 9888−9893. (f) Boussaad, S.; Tao, N. J. *J. Am. Chem. Soc.* **1999**, *121*, 4510−4515. (g) Immoos, C. E.; Chou, J.; Bayachou, M.; Blair, E.; Greaves, J.; Farmer, P. J. *J. Am. Chem. Soc.* **2004**, *126*, 4934−4942.
(6) (a) Kawahara, N. K.; Ohkubo, W.; Ohno, H. *Bioconjugate Chem.***1997**, *8*, 244−248. (b) Lvov, Y. M.; Lu, Z.; Schenkman, J. B.; Zu, X.; Rusling, J. F. *J. Am. Chem. Soc.* **1998**, *120*, 4073−4080. (c) Panchagnula, V.; Kumar, C. V.; Rusling, J. F. *J. Am. Chem. Soc.* **2002**, *124*, 12515−12521. (d) Liu, H.; Hu, N. *J. Phys. Chem. B* **2005**, *109*, 10464−10473.
(7) (a) Van Dyke, B. R.; Saltman, P.; Armstrong, F. A. *J. Am. Chem. Soc.* **1996**, *118*, 3490−3492. (b) Feng, M. Tachikawa, H. *J. Am. Chem. Soc.* **2001**, *123*, 3013−3020.
(8) Gao, Q.; Suib, S. L.; Rusling, J. F. *Chem. Commun.* **2002**, 2254−2255.
(9) Wang, Q.; Lu, G.; Yang, B. *Langmuir* **2004**, *20*, 1342−1347.
(10) (a) Topoglidis, E.; Cass, A. E. G.; Gilardi, G.; Sadeghi, S.; Beaumont, N.; Durrant, J. R. *Anal. Chem.* **1998**, *70*, 5111−5113. (b) Li, Q.; Luo, G.; Feng, J. *Electroanal.* **2001**, *13*, 359−363. (c) Topoglidis, E.; Campbell, C. J.; Cass, A. E. G.; Durrant, J. R. *Langmuir* **2001**, *17*, 7899−7906. (d) Grealis, C.; Magner, E. *Chem. Commun.* **2002**, 816−817.
(11) (a) Garwood, G. A.; Mortland, M. M.; Pinnavaia, T. J. *J. Mol. Catal.* **1983**, *22*, 153−159. (b) Kumar, C. V.; Chaudhari, A. *J. Am. Chem. Soc.* **2000**, *122*, 830−837. (c) Han, Y. J.; Watson, J. T.; Stucky, G. D.; Butler, A. *J. Mol. Catal. B: Enzymol.* **2002**, *17*, 1−5. (d) Xu, X.; Tian, B. Z.; Kong, J. L.; Zhang, S.; Liu, B. H.; Zhao, D. Y. *Adv. Mater.* **2003**, *15*, 1932−1936. (e) Peng, S.; Gao, Q.; Wang, Q.; Shi, J. *Chem. Mater.* **2004**, *16*, 2675−2684. (f) Shumyantseva, V. V.; Ivanov, Y. D.; Bistolas, N.; Scheller,. F. W.; Archakov, A. I.; Wollenberger, U. *Anal. Chem.* **2004**, *76*, 6046−6052.

10.1021/ac051640t CCC: $30.25
Published on Web 11/09/2005

microenvironment for enzyme loading and improve the stability of the entrapped enzymes. Mb in these films facilitated relatively faster electron transfer and catalytic activity than that between Mb in the solution and bare electrodes.[5−7,9] To date, most studies on immobilization of protein were focused on layered or mesoporous-structured materials due to their higher specific surface area.[11] In most cases, the reason for the interaction between the matrix and enzyme is not clear.

Titanium oxide anatase nanoparticles (TNP) were reported useful for the solar cell[12] and for the immobilization of heme protein and biomaterials in investigating spectroelectrochemical properties or bioanalytical applications.[10,13] Porous, nanostructured titanium oxide materials have found extensive applications in environmental purification, anode material for lithium rechargeable batteries, electronic devices, catalyst supports, gas sensors, and photovoltaic cells because of their remarkable chemical, electronic, and optical characteristics.[14] TiO_2 nanotubes have gradually received attention due to their one-dimensional nanostructures, uniform nanochannel, electronic conductivity, and larger specific surface area, which may greatly enhance their activity as catalysts or sensitivity as sensors.[15] Additionally, TiO_2 nanotubes are of chemical inertness, rigidity, and thermal stability, therefore, attractive for the development of nanotube biosensors. However, most work on TiO_2 nanotubes is still in the stage of synthesis process.[16] Titanate ($H_2Ti_3O_7$) nanotubes (TNT), composed of corrugated ribbons of edge-sharing TiO_6 octahedra,[17] were hydrothermally synthesized,[16a,16b] Although the electrochromism[18,19] of TNT film was recently reported, there are few reports in using these exciting nanotubes for biotechnology application. The titanate nanotubes are multilayered structures with a nanoscale inner core cavity and exposed to the outer surface,[20] which may provide a unique reaction vessel for analytes. $H_2Ti_3O_7$ contains a functional hydroxyl group; it is expected that the aqueous-like environment provided by the hydrophilic TNT surfaces will stabilize the immobilized proteins.[21] Furthermore, TNT ($H_2Ti_3O_7$) is a semiconductor material of layered structure[17,22] with H^+ ions distributed in the interlayer and surface of the nanotubes, which means that TNT is easily charged after treatment with bases. These interesting properties of TNT make it attractive to immobilize biomaterials and to keep their activity to a great extent. However, there are no reports describing utilization of metal oxide nanotubes to accommodate enzymes.

The study on redox protein immobilized in metal oxide nanotubes may help to understand the interaction mechanism between protein and membrane as well as to provide another way to enzyme engineering and, therefore, to explore biosensors with higher sensitivity. Herein we report an alternative strategy to use titanate nanotubes as efficient supports to immobilize Mb. For comparison, Mb encapsulated in TiO_2 anatase nanoparticles (TNP) film was also used. Mb almost retained its native secondary structures in TNT film, whereas Mb denatured to a great extent in TNP film. Mb entrapped in TNT film exerted facile direct electron transfer with the apparent heterogeneous electron-transfer rate constant (k_{ET}) of 86 ± 7 s^{-1}, ~ 4 times the 22 ± 5 s^{-1} value for Mb in the TNP membrane. In addition, the Mb−TNT membrane shows higher catalytic reactivity to oxygen and hydrogen peroxide. The Mb−TNT film shows the apparent Michaelis-Menton constant (K_M) of 140 μM and detection limit of 0.6 μM H_2O_2, greatly lower than those values for the Mb−TNP film. The possible mechanism for Mb stabilized and exhibited facile direct electron transfer in TNT film was proposed. Therefore, TNT has been proven to be an attractive matrix to accommodate heme protein and shows great promise to develop the nanotube-based third biosensor.

EXPERIMENTAL SECTION

Reagents. TNP (average size of ~6 nm, specific surface area of 341.2 m^2/g) was obtained from Ishihara Sangyo Kaisha, Ltd. (Osaka, Japan). Mb was purchased from Wako Chemical Co. (Tokyo, Japan). All the reagents were of the highest grade available and were used without further purification. All the solutions were prepared with Milli-Q water.

Synthesis of Titanate Nanotubes. Titanate ($H_2Ti_3O_7$) nanotubes (TNT) were prepared based on a published procedure[16a] with modification: TNP (1 g) and an aqueous solution of NaOH (10 M, 200 mL) were mixed and poured into a stainless Teflon-lined autoclave, then heated at 100 °C for 120 h. The white suspension was filtered and washed with dilute HCl and then deionized water until pH ~7 was attained. Finally, the product was dried.

Preparation of Colloidal Suspensions of TNT or TNP. A 25-mg aliquot of TNT powder was immersed in 0.1 M HNO_3 solution to replace the sodium ions with protons and was subsequently dispersed in 5 mL of 0.1 M tetraethylammonium hydroxide under stirring, resulting in a translucent suspension solution. This suspension was further diluted to 1 mg mL^{-1} TNT and adjusted to pH ~8 before use. The TNP suspension was prepared by dispersing a suitable amount of anatase TiO_2 nanoparticles in a similar way under stirring.

Fabrication of Mb−TNT or Mb−TNP Composite Film-Covered PG Electrode. Prior to coating, the basal plane pyrolytic graphite (PG) disk electrodes (3-mm diameter) were polished with 800-grit sandpaper, washed, and further sonicated in Milli-Q water. A mixture containing 0.1 mM Mb and 1 mg mL^{-1} TNT was sonicated for 15 min, and then a 10-μL aliquot of the thus-prepared TNT−Mb composite was uniformly cast onto the inverted PG disk

(12) (a) Nazeeruddin, M. K.; Kay, A.; Rodicio, I.; Humphry-Baker, R.; Mueller, E.; Liska, P.; Vlachopoulos, N.; Gratzel, M. *J. Am. Chem. Soc.* **1993**, *115*, 6382−6390. (b) Rensmo, H.; Keis, K.; Lindstrom, H.; Sodergren, S.; Solbrand, A.; Hagfeldt, A.; Lindquist, S.-E.; Wang, L. N.; Muhammed, M. *J. Phys. Chem. B* **1997**, *101*, 2598−2601.

(13) Meier, K. R.; Gratzel, M. *ChemPhysChem*. **2002**, *3*, 371−374.

(14) (a) Bach, U.; Lupo, D.; Comte, P.; Moser, J. E.; Welssörtels, F.; Scallbeck, J.; Spreitzer, H.; Grätezl, M. *Nature* **1998**, *395*, 583−585. (b) Wagemaker, M.; Kentgens, A. P.; Mulder, F. M. *Nature* **2002**, *418*, 397−399. (c) Zhou, H. S.; Li, D.; Hibino, M.; Honma, I. *Angew. Chem., Int. Ed.* **2005**, *44*, 799−802.

(15) (a) Beecroft, L. L.; Ober, C. K. *Adv. Mater.* **1995**, *7*, 1009−1012. (b) Patzke, G. R.; Krumeich, F.; Nesper, R. *Angew. Chem., Int. Ed.* **2002**, *41*, 2446−2461.

(16) (a) Kasuga, T.; Hiramatsu, M.; Hoson, A.; Sekino, T.; Niihara, K. *Langmuir* **1998**, *14*, 3160−3163. (b) Kasuga, T.; Hiramatsu, M.; Hoson, A.; Sekino, T.; Niihara, K. *Adv. Mater.* **1999**, *11*, 1307−1311. (c) Tian, Z. R.; Voigt, J. A.; Liu, J.; Mckenzie, B.; Xu, H. *J. Am. Chem. Soc.* **2003**, *125*, 12384−12385. (d) Sun, X.; Li, Y. *Chem. Eur. J.* **2003**, *9*, 2229−2238.

(17) Yao, B. D.; Chan, Y. F.; Zhang, X Y.; Zhang, W. F.; Yang, Z. Y.; Wang, N. *Appl. Phys. Lett.* **2003**, *82*, 281−283.

(18) Tokudome, H.; Miyauchi, M. *Chem. Commun*. **2004**, 958−959.

(19) Tokudome, H.; Miyauchi, M. *Angew. Chem., Int. Ed.* **2005**, 1974−1977.

(20) Chen, Q.; Zhou, W.; Chen, Q.; Du, G.; Peng, L. *Adv. Mater.* **2002**, *14*, 1208−1211.

(21) (a) Das, G.; Prabhu, K. A. *Enzyme Microb. Technol.* **1990**, *12*, 625−630. (b) Corma, A.; Fornes, V.; Rey, F. *Adv. Mater.* **2002**, *14*, 71−74.

(22) Ma, R.; Bando, Y.; Sasaki, T. *J. Phys. Chem. B* **2004**, *108*, 2115−2119.

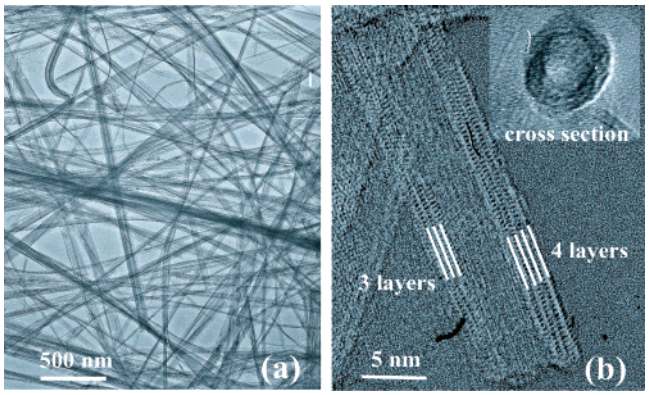

Figure 1. TEM images of prepared titanate nanotubes. (a) Low magnification; (b) high magnification. Cross section (inset).

electrode. In a similar way, the Mb−TNP-modified electrode was prepared by syringing a 10-μL aliquot of the prepared Mb−TNP suspensions (containing 0.1 mM Mb and 1 mg mL^{-1} TNP). In a control experiment, a matrix-only covered electrode was prepared by casting a 10-μL aliquot of TNT or TNP onto the PG electrode surface. These as-modified electrodes were dried under ambient conditions overnight before use.

Apparatus. Multipoint BET surface area of materials was calculated from the adsorption−desorption isotherm of N_2 at 77 K (Micromeritics ASAP 2010). Both transmission electron microscope (TEM) and scanning electron microscope (SEM) measurements were conducted using a JEM-2000EXII (JEOL Co. Ltd.) and a DS-720 (Topcon Co. Ltd.), respectively. The UV−visible absorption spectra of Mb, TNT, TNP, Mb−TNT, and Mb−TNP film-covered glass slides (after dry at room temperature overnight) were checked by using a UV3100 spectrophotometer (Shimadzu Co., Kyoto, Japan). FT-IR spectra for Mb, Mb−TNT, and Mb−TNP film-covered silicon wafers (after dry at room temperature overnight) were recorded with an FT-IR spectrophotometer (Jasco, Tokyo, Japan).

Electrochemical Measurements. The electrochemical response was measured in a conventional three-electrode system using a modified PG electrode as working electrode, a platinum wire as counter electrode, and a Ag/AgCl (3.3 M KCl) electrode as reference electrode. All potentials were reported in this context with respect to this reference. For cyclic voltammetry (CV) and square wave voltammetry (SWV) measurements, an Autolab potentiostat/galvanostat (Eco Chemie, B. V, Utrecht, The Netherlands) was used. The buffer solution was in thoroughly anaerobic conditions by bubbling with high-purity nitrogen. All measurements were performed at room temperature (~20 °C).

RESULTS AND DISCUSSION

Morphological Characterization of the Prepared Titanate Nanotubes. TNTs were synthesized by a hydrothermal process based on a published procedure[16a] with modification. The hollow nature of tubes with two ends open is clearly observed and a single nanotube is a three to four-layered wall with an intershell spacing of ~0.4 nm, and 4−5 nm in the inner diameter by TEM images (Figure 1). The specific surface area of TNT is 429.5 m^2/g. SEM images show that the nanotubes entangle with each other with typical lengths ranging from several hundreds nanometers to several micrometers (Supporting Information).

Morphological Characterization of TNT Film and TNP Film. From the viewpoint of structure, $H_2Ti_3O_7$ is a protonic titanate nature, which makes it possible to disperse TNT well in weak organic base such as alkylammonium. It is reported that TNT can be well dispersed in 0.1 M tetrabutylammonium hydroxide aqueous solution.[23] After treatment, TNT is in a colloidal state. In a similar treatment, TNPs are well dispersed. TNT film or TNP film was fabricated by casting 10-μL TNT or TNP suspensions on the PG electrode surface and drying at room temperature. Figure 2 shows SEM images of the TNT film and TNP film on the electrode surface. A typical cylindrical morphology with the barlike nanotubes was observed. The nanotubes are aggregated together to form a porous nanotubule layer on the electrode surface (Figure 2A). For TNP film, on the other hand, TiO_2 particles are randomly accumulated on the surface to form ill-ordered porous film. Some TiO_2 nanoparticles are aggregated into larger particles (Figure 2B).

Spectroscopic Characterization of Mb in TNT and TNP Film. The Soret band of heme protein is usually an indicator of the microenvironment where heme center locates. The peak will be diminished if the protein is denatured.[24] The band for Mb in TNT film is located at 414.6 nm, just a 2.6-nm red shift compared with that (412 nm) of native Mb film (Supporting Information). The Soret band shifts to 414.6 nm in TNT film may be due to the hydroxide-bound iron. The UV−visible absorption spectrum suggests that there is no obvious denaturation for Mb in TNT film. The Soret band of immobilized Mb in TNP film, on the other hand, is located at 398 nm, which is a 14-nm blue shift compared with that of native Mb film (Supporting Information). Also the absorbance is greatly decreased compared with that of native Mb film. This result indicates that there exists change in the vicinity of the heme center; thus, an apparent denaturation occurs for Mb in TNP film. In some situations, the immobilization of proteins at solid surfaces can result in the loss of native conformation to a great extent or denaturation of proteins.[25] FT-IR studies show the shapes of the amide I and amide II bands of Mb in the TNT membrane located at 1657.5 and 1543.7 cm^{-1}, respectively, which are essentially the same as those values (1656.6 and 1542.8 cm^{-1}) obtained from native protein (Supporting Information), indicating the actually undisturbed second structure for the bound protein in the Mb−TNT film. Comparably, the amide I and amide II bands of Mb in the TNP membrane are shifted to 1649.3 and 1530 cm^{-1}, respectively, strongly suggesting that the secondary structure of most Mb molecules was changed.

Electrochemical Characterization of Mb−TNT and Mb−TNP Films. Figure 3 shows typical cyclic voltammograms (CVs) of the TNT and Mb−TNT cast film-covered basal plane PG electrode (A) and the TNP and Mb−TNP cast film-covered PG electrode (B) in pH 5.5 buffer solution together. There are no redox peaks for TNT or TNP cast film-covered PG electrodes within the potential window (voltammogram a in Figure 3A and B). A well-defined, nearly reversible redox couple with the

(23) Ma, R.; Sasaki, T.; Bando, Y. *J. Am. Chem. Soc.* **2004**, *126*, 10382−10388.
(24) (a) George, P.; Hanania, G. *Biochem. J.* **1953**, *55*, 236−243. (b) Antonini, E.; Brunori, M. *Hemoglobin and myoglogin in their reactions with ligands*; North-Holland: Amsterdam, 1971; p 13. (c)Nassar, A.-E. F.; Willis, W. S.; Rusling, J. F. *Anal. Chem.* **1995**, *67*, 2386−2392.
(25) Torii, H.; Tasumi, M. In I*nfrared Spectroscopy of Biomolecules*; Mantsh, H. H., Chapman, D., Eds.; Wiley: New York, 1996; pp 1−18.

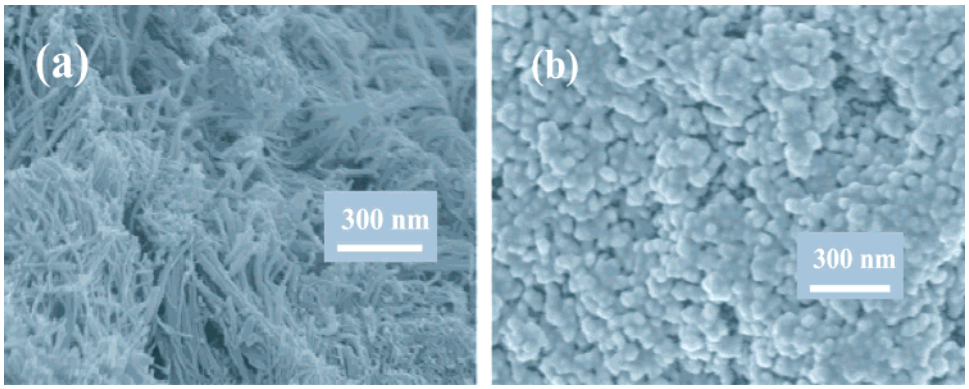

Figure 2. SEM images of TNT film (a) and TNP film (b).

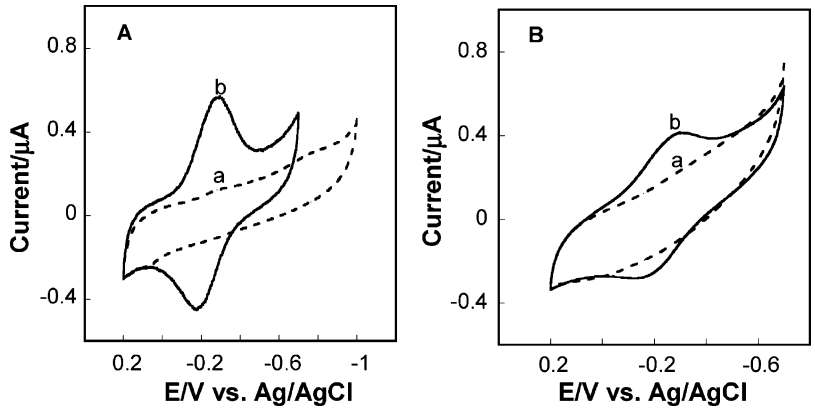

Figure 3. (A) Cyclic voltammograms of TNT (a) and Mb−TNT film (b)-covered PG electrode. (B) Cyclic voltammograms of TNP (a) and Mb−TNP film (b)-covered PG electrode. Cyclic voltammograms were measured in 0.1 M HAc−NaAc buffer solution (pH 5.5). Scan rate, 0.1 V s^{-1}.

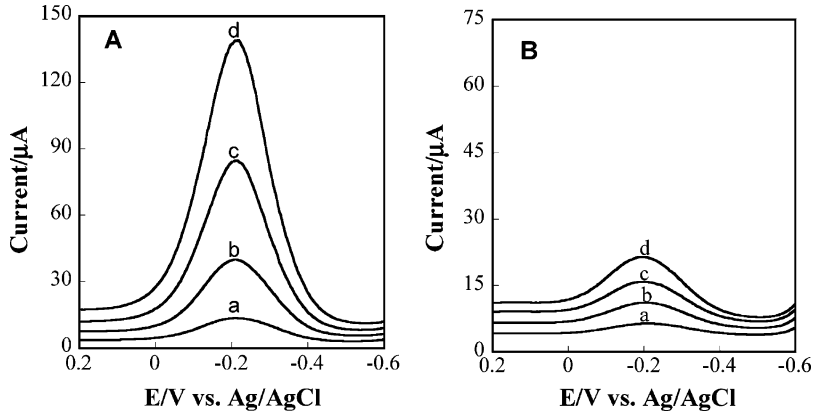

Figure 4. Square wave voltammograms of Mb−TNT film (A) and Mb−TNP film-covered PG electrode (B) in 0.1 M HAc−NaAc buffer solution (pH 5.5). SWV conditions: equilibration time, 5 s; potential amplitude, 100 mV; step height, 4 mV; and frequency, 25 (a), 50 (b), 75 (c), and 100 Hz (d).

apparent formal peak potential (E_p) of −0.239 V was observed for the Mb−TNT composite-covered PG electrode (voltammogram b in Figure 3A), indicating that the direct electron transfer of Mb is achieved through the incorporation into TNT film. Here E_p is defined as the average value of the anodic peak potential (E_{pa}) and the cathodic peak potential (E_{pc}); that is, $E_p = (E_{pa} + E_{pc})/2$. Both the cathodic peak current (i_{pc}) and the anodic peak current (i_{pa}) increase linearly with the scan rate up to 5 V s^{-1} (Supporting Information), which is characteristic of thin-layer electrochemistry;[26] that is, almost all electroactive met-Mb in the membrane is converted to oxy-Mb on the forward CV sweep and vice verse. The ratios of i_{pc} to i_{pa} are within 0.98−1.02, very close to the value of unity expected when there are no kinetic or other complications in the electrode process. The Mb−TNP-covered PG electrode (voltammogram b in Figure 3B), on the other hand, shows a quasi-reversible wave with E_p of −0.263 V. The electron transport mechanism for Mb in TNP film is a function of scan rate; that is, it exhibits thin-layer behavior at lower scan rates (lower than 0.6 V s^{-1}), while diffusion-controlled behavior is demonstrated at scan rates above 1 V s^{-1} (Supporting Information). Similar behavior was observed for Mb immobilized in surfactant film.[5g] The total amount of Mb

(26) Bard, A. J.; Faulkner, L. R. *Electrochemical Methods. Fundamentals and Applications*, 2nd ed.; Wiley: New York, 2001.

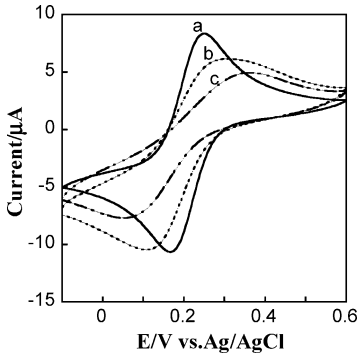

Figure 5. Cyclic voltammograms of bare PG (a), TNP cast PG (b), and TNT cast PG (c) electrode in 0.1 M phosphate buffer solution (pH 7.2) containing 1 mM $K_3[Fe(CN)_6]$. Scan rate, 0.05 V s^{-1}.

on the TNT-Mb-film covered electrode surface is calculated to be ~1 nmol. By integration of the anodic peaks in CV, the charges and thus the average surface concentration of electroactive speciescan be calculated. The average surface concentration of electroactive Mb in TNT film was estimated to be 2.0 nmol cm^{-2}, accounting for ~15% of the total amount of Mb on the electrode surface. On the other hand, the average surface concentration of electroactive Mb in TNP film was 1.3 nmol cm^{-2}, accounting for ~10% of the total amount of Mb on the electrode surface.

The electron transfer of Mb within the TNT film was further studied by square wave voltammetry (SWV). SWV is known to be powerful in characterizing the electrochemistry of interfacially confined redox species.[27] Typical square wave voltammetry (SWVs) of Mb−TNT and Mb−TNP film are depicted in Figure 4. A better resolution and signal-to-noise ratio was obtained. On the basis of a nonlinear regression analysis program, which was derived from the theory for SWV of a surface-confined species of apparent standard potential values, the apparent heterogeneous electron-transfer rate constant (k_{ET}) can be calculated.[28] The k_{ET} values for Mb in TNT and TNP film were estimated to be 86 ± 7 and 22 ± 5 s^{-1}, respectively, based on the program reported.[28c] In context, the k_{ET} values for Mb immobilized in some surfactant films were reported to be within 30−59 s^{-1}.[5d] Clearly, Mb shows a higher electron-transfer rate constant in TNT film than that in TNP film and other films.

Possible Mechanism That Mb Stabilized and Exhibited Improved Direct Electrochemistry in TNT Film. Mild conditions are prerequisites for proteins' retention of their native structure and activity. The specific surface area of TNT (429.5 m^2/g) is just 26% larger than that (341.2 m^2/g) of TNP, which should not be attributed much to the difference of accommodation of the Mb. Both of the surfaces of TNT and TiO_2 nanoparticles are covered with hydroxyl groups.[29] In the case of TiO_2 nanoparticles, however, the principal amphoteric surface functionality is the "titanol" moiety, >TiOH,[29] which is quite different from the hydroxyl group of $H_2Ti_3O_7$ in TNT.[20,30] It is expected that the hydrophilic nature will provide an aqueous-like microenvironment to stabilize the immobilized proteins.[21] $H_2Ti_3O_7$ is a protonic acid; therefore, the nanotubes are in a colloidal state with the negatively charged surface after treatment with a weak organic base.[23,30] This is supported by comparison of the electrochemical responses of ferri/ferrocyanide at TNT cast electrode and TNP cast electrode (Figure 5). At the TNT cast electrode, a severe decrease in the redox peak and a great widening of the peak-to-peak separation (ΔE_p) was observed, which is due to the electrostatic repulsion between $Fe(CN)_6^{3-}$or $Fe(CN)_6^{4-}$ anion and the negatively charged TNT surface. At the TNP cast electrode, on the other hand, the redox peak was not so much disturbed compared with that at the bare electrode. This result suggests that the TNT surface is more negatively charged. In the context, a similar report was shown for the negatively charged surface.[31] Below pH 7, Mb has a net positive charge.[32] It is reasonable that the positively charged proteins show higher affinity for the anionic TNT surface than for the TiO_2 nanoparticle. Thus, the electrostatic attractions should be responsible for Mb accommodation in the TNT film. Moreover, Some Mb (size of 2.5 × 3.5 × 4.5 nm[33]) molecules can be encapsulated into the two-end opened nanochannels (4−5 nm in diameter) of TNT.[20] These factors will favor the accommodation of Mb and retention of its activity. This cannot be expected for TiO_2 nanoparticles. A model for Mb accommodation is illustrated in Scheme 1A.

Though the exact reason for Mb-exhibited enhanced direct electrochemistry in the TNT film is unclear yet, it probably arises from the unique specialty of the advantages of the titanate nanotubes. TNT is a semiconductor material of layered structure.[17] H^+ ions are distributed in the interlayer and surface of TNT ($H_2Ti_3O_7$).[16c,17,30] It is reasonable that H^+ ions on the TNT surface may take part in the Fe^{2+}/Fe^{3+} redox process for Mb. The reaction is expressed in eq 1.[34]

$$Mb(Fe^{3+}) + H^+ (TNT) + e^- \rightleftharpoons Mb(Fe^{2+})H(TNT) \quad (1)$$

Therefore, more Mb molecules in the TNT membrane are in the right orientation for electron-transfer relay. A possible mechanism for Mb facilitating the improved electron transfer in TNT film is shown in Scheme 1B.

Electrocatalytic Property of Mb−TNT and Mb−TNP Electrodes. Electrocatalytic reduction of hydrogen peroxide was examined by measuring CVs using the Mb−TNT or Mb−TNP

(27) Reeves, J. H.; Song, S.; Bowden, E. F. *Anal. Chem.* **1993**, *65*, 683−688.
(28) (a) O'Dea, J. J.; Osteryoung, J. G. *Anal. Chem.* **1993**, *65*, 3090−3097. (b) Zhang, Z.; Rusling, J. F. *Biophys. Chem.* **1997**, *63*, 133−146. (c) Fan, C.; Wang, H.; Sun, S.; Zhu, D.; Wagner, G.; Li, G. *Anal. Chem.* **2001**, *73*, 2850−2854.
(29) Hoffmann, M. R.; Martin, S. T.; Choi, W.; Bahnemann, D. W. *Chem. Rev.* **1995**, *95*, 69−96.
(30) Ma, R.; Bando, Y.; Sasaki, T. *Chem. Phys. Lett.* **2003**, *380*, 577−582.
(31) Liu, A.; Anzai, J. *Anal. Chem.* **2004**, *76*, 2975−2980.
(32) Friend, S. H.; Gurd, F. R. N. *Biochemistry* **1979**, *18*, 4612−4619.
(33) Kendrew, J. C.; Dickerson, R. E.; Strandberg, B. E.; Hart, R. G.; Davies, D. R.; Phillips, D. C.; Shore, V. C. *Nature* **1960**, *185*, 422−427.
(34) (a) The potential of the $Mb(Fe^{3+})/Mb(Fe^{2+})$ redox pair was linearly negatively shifted with the increasing pH of buffer solution, indicating that the direct electrochemistry of Mb in TNT film is highly pH-dependent (Supporting Information). The slope of the line is −53 mV/pH, which is near the optimal value of the −58 mV/pH at 20 °C for a one-proton transfer coupled with reversible one-electron transfer, suggesting that one proton participated in a single electron-transfer process to neutralize the excess charge that accumulated at the electrode surface upon electrochemical reduction. See: Bond, A. M. *Modern Polarographic Methods in Analytical Chemistry*; Marcel Dekker: New York, 1980; pp27−31. (b) The pH dependence of the potential of $Mb(Fe^{3+})/Mb(Fe^{2+})$ pair is in agreement with the assumption that some Mb in TNT film is probably hydroxide-bound above pH 7.

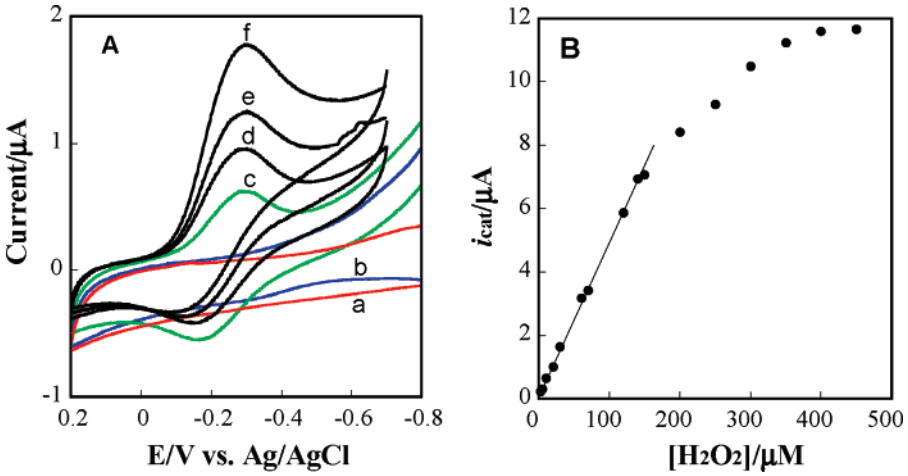

Figure 6. (A) Cyclic voltammograms of the TNT cast PG electrode in 0 μM (a) and 150 μM H_2O_2 (b). Cyclic voltammograms of the Mb−TNT film-covered PG electrode in the presence of 0 (c), 5 (d), 10 (e), and 20 μM H_2O_2 (f). Cyclic voltammograms were measured in 0.1 M HAc−NaAc buffer solution (pH 5.5). Scan rate, 0.2 V s^{-1}. (B) Typical plot of the electrocatalytic current (i_{cat}) versus H_2O_2 concentration for the Mb−TNT electrode.

Scheme 1. (A) Model for Mb Accommodation in TNT. (B) Possible Mechanism for Mb Exhibition of Facile Electron Transfer with TNT Film

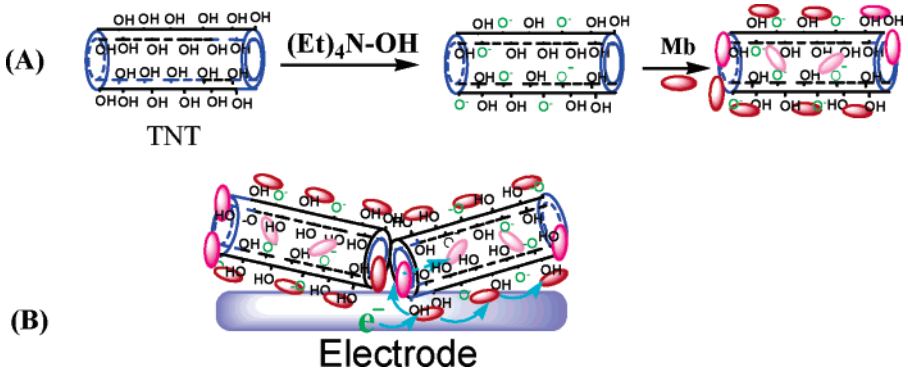

film-modified electrode. Figure 6A shows CVs of the Mb−TNT film-modified electrode and TNT-covered electrode in the absence or the presence of H_2O_2. The cathodic peak (~ −0.3V) was greatly enhanced in the presence of H_2O_2, while the corresponding anodic peak decreased, suggesting that an electrocatalytic reduction of H_2O_2 occurred (Figure 6A). The i_{pc} value increases with the increasing concentration of H_2O_2 added. No peaks were observed at the TNT cast electrode in the presence of H_2O_2. The electrocatalytic current (i_{cat}) linearly increased with increasing concentration of H_2O_2 in the beginning and thereafter began to level off (Figure 6B), suggesting that the immobilized enzyme responds to the presence of the substrate in a Michaelis−Menten model. Here the i_{cat} value is defined as the difference between i_{pc} in the presence of H_2O_2 and i_{pc} in the absence of H_2O_2 for the Mb−TNT electrode. The i_{cat} values are linear with increasing concentration of H_2O_2 in the range of 2−160 μM for the Mb−TNT electrode. The lower detection limit is 0.6 μM H_2O_2 for the Mb−TNT electrode (S/N = 3). The Lineweaver−Burke plot shows an apparent Michaelis−Menten constant (K_M) of 140 μM for the Mb−TNT electrode. Identical experiments were performed using the Mb−TNP electrode, and their analytical performances were collected in Table 1. For comparison, other reported protein films were also listed in Table 1. In contrast with the Mb−TNP film and other films reported so far,[6d,11e,35,36] the Mb−TNT film presents excellent analytical performance in the determination of H_2O_2, for instance, lower detection limit and wider linear range. The Mb−TNT film demonstrates a smaller K_M value, indicating that Mb entrapped in TNT film shows higher peroxidase-like activity.

Table 1. Peroxidase-like Activity of Some Protein Films

film	detection range/μM	detection limit/μM	k_M/μM	ref
Mb−titanate nanotubes	2−160	0.6	140	*a*
Mb−nanocrystalline TiO_2	6−80	3.0	1300	*a*
HRP−silica sol−gel	20−2600	na[b]	4800	35
Mb−ziroconium phosphonates	na	na	440	36
Mb−$CaCO_3$ multilayer	5−80	2.0	56	6d
Mb−magadiite nanocomposite	na	na	350	11e

[a] Present work. [b] na, not available.

CONCLUSIONS

A comparative study of titanate nanotubes and TiO_2 anatase nanoparticles as support matrix for the immobilization of myo-

(35) Li, J.; Tan, S. N.; Ge, H. *Anal. Chim. Acta* **1996**, *335*, 137−145.
(36) Bellezza, F.; Cipiciani, A.; Costantino, U.; Nicolis, S. *Langmuir* **2004**, *20*, 5019−5025.

globin was carried out. Mb almost retained its native secondary structures in TNT film, whereas Mb denatured to a great extent in TNP film. Myoglobin exhibits facile direct electrochemistry in titanate nanotube film than in nanocrystalline TiO_2 film. Mb entrapped in titanate nanotube film exerted facile direct electron transfer with the apparent heterogeneous electron-transfer rate constant (k_{ET}) of $86 \pm 7\ s^{-1}$, ~4 times the $22 \pm 5\ s^{-1}$ value for Mb in nanocrystalline TiO_2 membrane. In addition, the Mb−TNT membrane demonstrates higher catalytic reactivity to oxygen and hydrogen peroxide. The Mb−TNT film shows the apparent Michaelis−Menton constant (K_M) of 140 μM and detection limit of 0.6 μM H_2O_2, much lower than those values for the Mb−TNP film. Therefore, the present study strongly suggests that titanate nanotubes are excellent matrixes for myoglobin to exhibit efficient direct reversible electron transfer and higher catalytic activity to hydrogen peroxide. The hydroxyl group, the surface charge, and the tubular morphology of TNT play important roles in stabilizing the bound protein. This methodology described here can be applicable to preparing titanate nanotube-based third-generation biosensors and protein characterization. Also it paves a way to study other metal oxide nanotubes as promising supports for many biological events where biomacromolecules are involved.

ACKNOWLEDGMENT

A.L. gratefully acknowledges Japan Society for the Promotion of Science (JSPS) for the financial support of this work.

SUPPORTING INFORMATION AVAILABLE

SEM images of titanate nanotubes, UV−visible spectra, FT-IR spectra, plots of peak current versus scan rate, plot of peak potential versus solution pH, and the electrocatalytic reduction of oxygen by the Mb−TNT film-covered PG electrode. This material is available free of charge via the Internet at http://pubs.acs.org.

Received for review September 14, 2005. Accepted October 14, 2005.

AC051640T